scientific reports

Check for updates

OPEN

METTL10 attenuates adriamycin-induced podocyte injury by targeting cell dedifferentiation

Jiwen Bao[1,2], Ziyang Li[1], Huanzhen Yao[1], Bei Wu[1], Leyi Gu[1], Yangbin Pan[2] & Ling Wang[1]✉

Chronic kidney disease (CKD) is a worldwide public health problem. Podocyte damage is a hallmark of glomerular diseases including focal segmental glomerulosclerosis (FSGS) and one of the leading causes of CKD. Lysine methylation is a crucial post-translational modification. Beyond epidemic regulation, various lysine methyltransferases have been recently reported to participate in disease progression, including cancers and kidney diseases. Among them, Methyltransferase-like 10 (METTL10), is recognized as a gene associated with estimated glomerular filtration rate (eGFR) and CKD risk. However, its role in podocyte damage remains unclear. We identified the differentially expressed genes(DEGs)in podocyte injury by bioinformatics analysis. Patients diagnosed as idiopathic FSGS by renal biopsy were enrolled. Mouse model was established by Adriamycin(ADR) and urinary albumin/ creatinine ratio(UACR) was detected. Murine podocyte cell line was stimulated with ADR. We determined METTL10 was one of the significantly downregulated genes in damaged podocytes, confirmed the decreased glomerular expression of METTL10 in patients with idiopathic FSGS and in mice with ADR-induced nephrosis, respectively. Moreover, we found a negative correlation between glomerular METTL10 levels and UACR in mice. METTL10 was reduced in ADR-treated podocytes, accompanied by podocyte dedifferentiation (loss of synaptopodin, podocin, nephrin, WT-1) and acquisition of mesenchymal cell markers (snail, desmin, pax2). Knockdown of METTL10 promoted their dedifferentiation. METTL10 regulates podocyte dedifferentiation under damaging stimuli and protects podocytes.

Keywords FSGS. METTL10. podocyte.dedifferentiation. Adriamycin(ADR)

Chronic kidney disease (CKD) is recognized as a worldwide public health problem with increasing prevalence, poor outcomes and high treatment costs, affecting 12% of all adults in the United States and 10.8% in China[1]. The burden of CKD has implications for the demand for renal replacement therapy and is associated with a higher risk of morbidity, mortality, and hospitalization[2].

Podocytes are terminally differentiated visceral epithelial cells of the glomerulus that express specific podocyte differentiation markers and lack the ability to proliferate[3]. As the indispensable components of glomerular filtration barrier, podocytes play a critical role in the pathomechanism of proteinuric kidney diseases, including minimal change disease (MCD), focal segmental glomerulosclerosis (FSGS), membranous nephropathy (MN), and diabetic nephropathy (DN)[4]. The majority of such podocyte disorders are progressive in nature leading to CKD and even end stage kidney disease(ESRD)[5]. However, the insufficiency of pratical and effective interventions on podocyte injury demands a better and deeper understanding of the crucial and universal molecules involved in varied podocyte disorders[6].

Adriamycin (ADR), one of the most widely used chemotherapeutic drug, is also a well-known toxic agent of renal injury, which mimics histological changes and causes proteinuria that are observed in human CKD due to primary FSGS[7]. Histologically, ADR can induce podocyte damage and thinning of the glomerular endothelium, further causing a constant delete of podocyte numbers and the development of progressive FSGS in certain mice strains[8].Therefore, ADR is frequently used to establish experimental FSGS mouse model.

Protein lysine methylation is a crucial post-translational modification(PTM) that regulates the functions of both histone and non-histone proteins. Over the past decades, there are a growing body of lysine methyltranfereses (KMTs) subsequently identified and implicated in the progression of various diseases including cancers and kidney diseases, among which, enhancer of zeste homologue 2 (EZH2) and disruptor of telomeric silencing

[1]Department of Nephrology, Ren Ji Hospital, Shanghai Jiao Tong University School of Medicine, Shanghai, China. [2]Department of Nephrology, Shanghai Pudong Hospital, Fudan University, Pudong Medical Center, Shanghai, China. ✉email: shwangling@126.com

1-like protein (DOT1L) have been most extensively characterized as drug targets and their inhibitors have been tested in the clinic[9]. Similarly, the novel KMTs, such as Methyltransferase-like 3(*METTL3*), Methyltransferase-like 7(*METTL7*), Methyltransferase-like 14(*METTL14*) and SET domain-containing protein 2 (*SETD2*) are characterized as the commonly mutated genes in renal cell carcinoma(RCC)[10-11]. Moreover, increasingly amounts of reseaches have indicated these METLL family members are linked to different types of kidney diseases, containing not merely acute kidney injury(AKI), but podocyte disorders. For instance, Zhihui Lu and et al. indicated that METTL 14, as a KMT for N6-methyladenosine(m6A) in eukaryotic mRNA, aggravates podocyte injury and FSGS progression through promoting Sirt1 mRNA m6A modification[12].

Methyltransferase-like 10 (METTL10) is a lysine trimethyltransferase targeting eukaryotic translation elongation factor 1A1 (eEF1A1), which is well preserved from simple eukaryotes such as Saccharomyces cerevisiae to mammals such as humans and mice[13-14]. Recently, *METTL10*was identified as an estimated glomerular filtration rate (eGFR)-associated gene through a transethnic genome-wide association study of eGFR[15]. Furthermore, several studies have reported that *METTL10*is one of the putative CKD risk genes[16]. Considering the fact that many METTLs are found to participate in the progress of podocyte disorders, we hypothesized that METTL10 might play a role in podocyte injury in a similar way.

In the present study, we demonstrate for the first time that METTL10 is associated with FSGS and alleviates ADR-induced podocyte injury by targeting cell dedifferentiation, suggesting that METTL10 may be a novel protective molecule for podocytes.

Results

METTL10 was downregulated in podocyte injury as shown by bioinformatics analysis

A total of 5353 genes were significantly differentially expressed in damaged podocytes compared with normal podocytes. (Fig. 1a) As shown in the volcano plot, 1951 DEGs were downregulated and 3402 DEGs were upregulated in injured podocytes compared with intact podocytes. Here, we show some examples of DEGs in

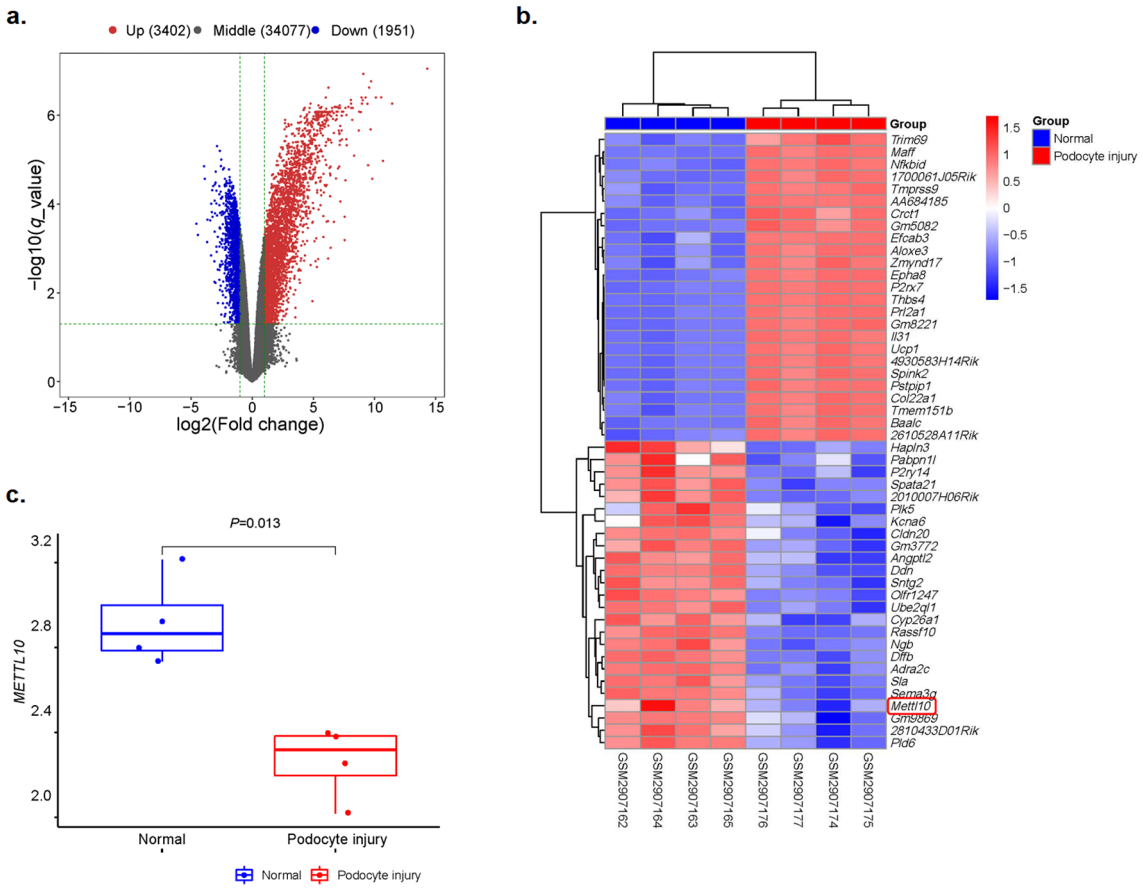

Fig. 1. METTL10 was downregulated in podocyte injury by bioinformatic analysis. (a) Volcano plot of differentially expressed genes (DEGs) specific to podocyte injury. Genes with a significant change of more than twofold were selected. Red spots show the upregulated genes, blue spots are downregulated genes, and black spots represent nonsignificantly expressed genes. (b) Examples of DEGs are shown in the heatmap. Red areas represent highly expressed genes, and blue areas represent genes expressed at low levels in damaged podocytes compared with normal podocytes. (c) METTL10 was one of the downregulated key genes in damaged podocytes compared with intact podocytes.

podocyte injury. (Fig. 1b) Surprisingly, we found that *METTL10* was one of the significantly downregulated DEGs in the podocyte injury group compared with the normal group ($P<0.05$). (Fig. 1c)

Downregulation of METTL10 in the kidneys of patients and an adriamycin-induced mouse model

Adriamycin (ADR)-induced nephropathy is widely applied as the leading model to study human primary.

focal segmental glomerulosclerosis (FSGS)[17]. Therefore, to confirm the differential expression of METTL10 inpodocyte injury, we examined METTL10 expression by immunostaining and immunoblotting in validation cohorts of individuals with FSGS and mice with ADR-induced nephrosis. For the human studies, we examined archived kidney tissue from a cohort of patients without pathological abnormalities ($n=4$) and from patients with massive proteinuria and confirmed FSGS ($n=6$). The clinical characteristics of these patients are described in Table 3. Patients in the FSGS group had nephrotic-range proteinuria (> 3.5 vs. <0.5 g/24 h) and significantly lower levels of serum albumin (26.06 ± 7.07 vs. 42.78 ± 7.15 g/L, $P<0.01$) than the control patients. However, the characteristics, including age, BP, BUN, creatinine and eGFR, were not significantly different between the two groups. We observed an approximate doubling of METTL10 and podocalyxin in the glomeruli of the control group. Moreover, the expression of METTL10 was decreased in patients with FSGS compared with control patients. (shown in Fig. 2a)

For the mouse study, we examined kidney tissue from ADR-induced nephrotic mice and normal mice ($n=4$ per group) aged 6–8 weeks. Compared with that of the control mice, effacement of foot processes appeared in the mice with ADR-induced nephrosis at 14 days. (shown in Fig. 2b) The immunoblotting assay revealed that METTL10 protein expression was significantly downregulated by 59.48 ± 12.00% in mouse kidneys with ADR treatment compared with the controls ($P<0.01$). The expression of the podocyte-specific markers synaptopodin, nephrin, Wilms' tumor 1 (WT1) and podocin was significantly decreased by 46.65 ± 14.37%($P<0.05$), 38.72 ± 14.69%($P<0.05$), 47.51 ± 11.44%($P<0.01$), and 72.49 ± 6.84%($P<0.0001$), respectively. (shown in Fig. 2c-d). As shown in Fig. 2e, we found that the urinary albumin/creatinine ratios of the control group on Day 0 and Day 14 were 175.2 ± 44.47 and 267.2 ± 41.13 mg/mmol, respectively. The urinary albumin/creatinine ratios of the ADR-treated group were 162.9 ± 19.66 and 1503 ± 238.2 mg/mmol, respectively. After 14 days of ADR injection, mice developed gross proteinuria. Notably, the level of METTL10 in the glomeruli was negatively correlated with the urinary albumin/creatinine ratio. (shown in Fig. 2f)

METTL10 was reduced in cultured podocytes stimulated with ADR

We further validated the changes in METTL10 in an in vitro study using ADR to stimulate mature podocytes. As Fig. 3a shows, METTL10 localized to the nucleus and cytosol of podocytes, which is consistent with other studies[18]. After treatment with ADR (0.25 μg/ml) for 48 h, the protein expression of METTL10 was also significantly downregulated by 46.92 ± 11.3%($P<0.01$) in podocytes, along with reductions in WT1 (33.57 ± 7.78%, $P<0.01$)) and podocin (29.05 ± 10.31%, $P<0.05$), compared with that of the control group. (shown in Fig. 3b, c)

In addition, as shown in Fig. 4a, real-time PCR analysis revealed that after stimulation with ADR for 4 h, the levels of dedifferentiated-related genes, including desmin, snail2 and pax2, were increased by 39.48 ± 8.44%, 47.25 ± 11.95% and 77.60 ± 18.82%, respectively, while the mRNA level of WT1 was decreased by 31.40 ± 10.35% compared with the controls. After ADR treatment for 6 h, the mRNA expression of METTL10 was also downregulated by 15.85 ± 3.94%, the expression of desmin and snail2 reached 142.50 ± 8.15% and

Gene product	Primer sequences	Accession number/references	size of products
METTL10	Forward: CCCATTGGATGCCTCAGTGCTTG	NM_028095.1	23
	Reverse: AACTTGGGTGTTGGCAGCTCTTC		23
WT1	Forward: TCTTCCGAGGCATTCAGGATG	NM_144783.2	21
	Reverse: TGCACACATGAAAGGACGTTT		21
Synaptopodin	Forward: AGCAAGTGAAAGAAGCAAAGTCT	NM_177340.2	23
	Reverse: CAGTACCGTAACTGACTAGGGT		22
Desmin	Forward: GTGGATGCAGCCACTCTAGC	NM_010043.2	20
	Reverse: TTAGCCGCGATGGTCTCATAC		21
Snail2	Forward: TGGTCAAGAAACATTTCAACGCC	NM_011415.3	23
	Reverse: GGTGAGGATCTCTGGTTTTGGTA		23
Snail3	Forward: CACACGCTGCCTTGTGTCT	Xie, K. et al. Yes-Associated Protein Regulates Podocyte Cell Cycle Re-Entry and Dedifferentiation in Adriamycin-Induced Nephropathy. Cell Death Dis. 10, 915 (2019).	19
	Reverse: GGTCAGCAAAAGCACGGTT		19
PAX2	Forward: AAGCCCGGAGTGATTGGTG	NM_001368743.1	19
	Reverse: CAGGCGAACATAGTCGGGTT		20
GAPDH	Forward: CCAATGTGTCCGTCGTGGATCT	NM_008084.4	22
	Reverse: GTTGAAGTCGCAGGAGACAACC		22

Table 1. Oligonucleotides used in real-time PCR for the selected genes.

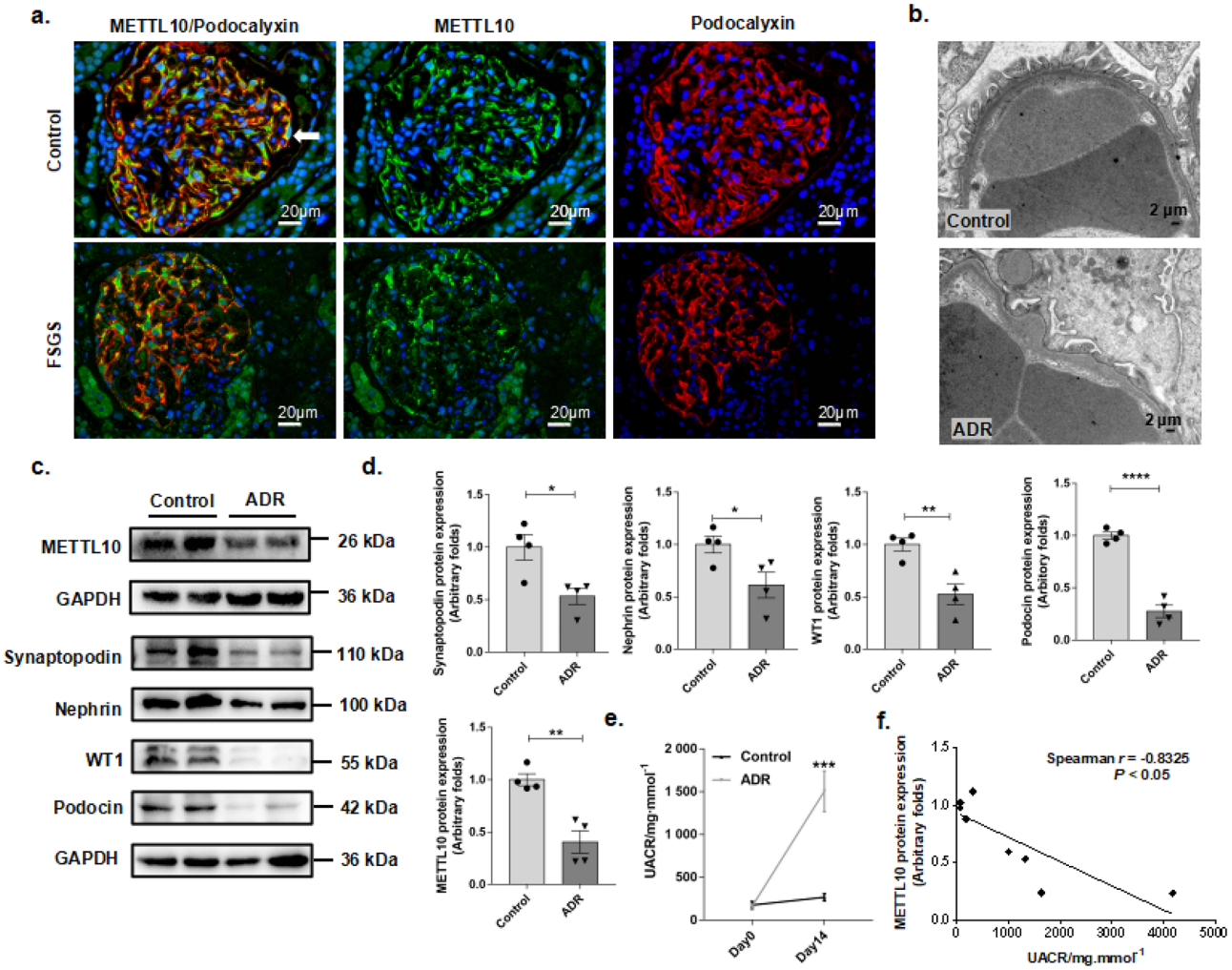

Fig. 2. Decrease in METTL10 in humans and mice. (a) Immunofluorescence staining of METTL10 in the kidneys of patients with FSGS compared with controls; the white arrow indicates colocalization of METTL10 (green) and podocalyxin (red) (magnification, ×400). (b) Effacement of foot processes was observed at 4 weeks after adriamycin (ADR) injection. (c) Western blot analysis of glomeruli from ADR-treated mice. (d) Bar graph of c. ($n=4$, $^{**}P<0.01$, $^{***}P<0.001$, $^{****}P<0.0001$). (e) Urine albumin creatine ratio (UACR) in control mice and ADR-treated mice; error bars indicate the SEM ($n=3$, $^{***}P<0.001$). (f) Correlation between the relative protein levels of METTL10 in the glomeruli and UACR in all mice ($n=8$).

160.80 ± 4.31%, respectively, and the WT1 gene expression decreased to 35.76 ± 5.22% of that in the control group. (shown in Fig. 4b)

METTL10 alleviated adriamycin-induced injury of podocytes

Podocytes are vulnerable to a variety of injurious stimuli, such as ADR, hyperglycemia, and transforming growth factor β (TGFβ)[19–21]. In response to these stimuli, podocytes can undergo a range of changes involving dedifferentiation (mesenchymal transition), hypertrophy, autophagy, mitotic catastrophe, detachment and apoptosis[22–24].

Here, we found an association between METTL10 and podocyte dedifferentiation, a maladaptive response of podocytes to various stressful stimuli[23]. We genetically upregulated the expression of METTL10 in podocytes by lentivirus infection and examined the impact on ADR-induced podocyte impairment. As shown in Fig. 5a-b, the decreased expression of podocin in ADR-treated podocytes, which is exclusively expressed in podocytes[25], was in part restored by overexpression of METTL10.

Furthermore, podocytes were transfected with METTL10-inhibiting RNA (siRNA). Forty-eight hours after transfection, the expression of METTL10 protein was downregulated by 59.7 ± 14.01% compared with that in the negative control group. (Fig. 5c-d). Moreover, the protein levels of synaptopodin and nephrin, both podocyte-specific markers, were decreased by 77.31 ± 17.43% and 46.73 ± 16.32%, respectively. The dedifferentiation-associated proteins desmin and snail2 were significantly upregulated by 125.0 ± 44.28%($P<0.01$) and 110.1 ± 13.83%($P<0.05$), respectively, after METTL10 knockdown. Similarly, the mRNA level of synaptopodin in the METTL10 knockdown group was reduced by 22.95 ± 4.35%, accompanied by the upregulation of

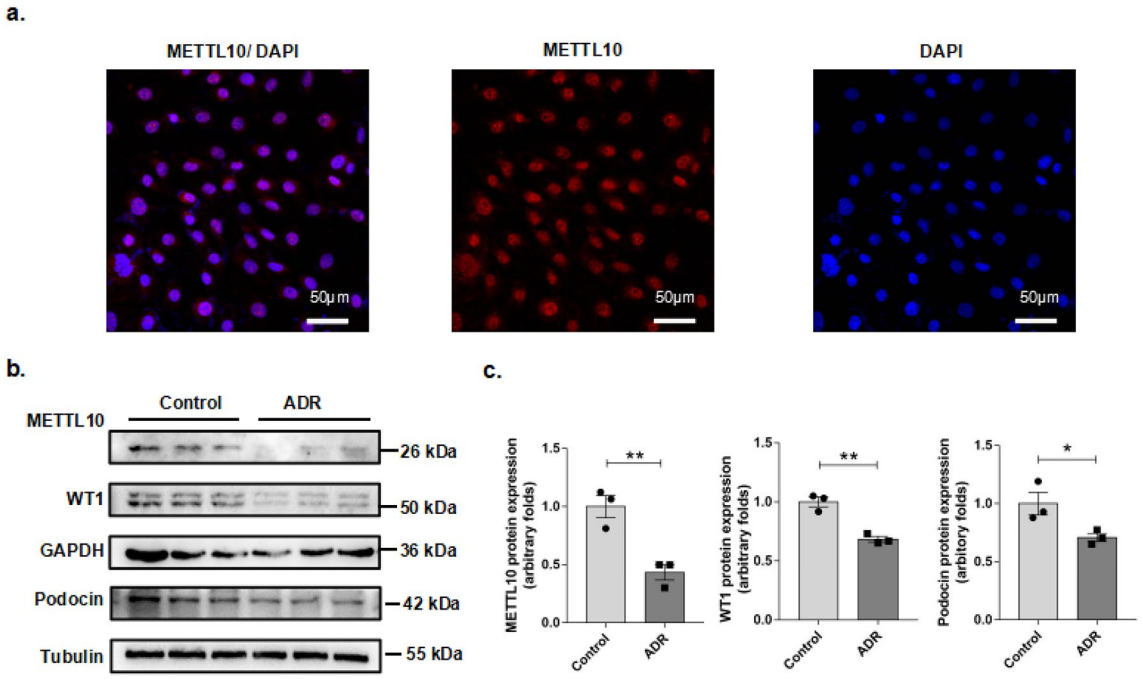

Fig. 3. METTL10 was reduced in podocyte injury induced by ADR. (a) Immunofluorescence staining for subcellular localization of METTL10 in podocytes (magnification, ×400). (b) Western blot analysis of podocytes treated with ADR (0.25 μg/mL) for 48 h. (c) Immunoblotting quantification of (b). $n = 3$ per group. Each bar represents data obtained from at least three independent experiments. $^{*}P < 0.05$, $^{**}P < 0.01$, $^{***}P < 0.001$. CON control, ADR adriamycin.

dedifferentiation-related mRNAs such as desmin (30.36 ± 5.53%), snail2 (36.90 ± 12.44%), snail3 (45.30 ± 6.41%) and pax2 (61.42 ± 9.27%). (shown in Fig. 4c) Therefore, knockdown of METTL10 may promote dedifferentiation of podocytes.

Discussion

Podocyte injury is widely known as one of the key determinants in the progression of proteinuric kidney diseases[26]. Identifing the underlying mechanism of podocyte injury is obviously significant for exploring new effective therapeutic strategies on podocytopathies[5].

Lysine methylation is known as a vital posttranslational modification that regulates the functions of both histone and nonhistone proteins, DNA and RNA[27]. Accumulating evidence has shown that lysine methyltransferases (KMTs) play important roles in various organ diseases, including kidney disease[28]. For instance, EZH2, a lysine trimethyltransferase at lysine residue 27 on histone protein H3 (H3K27me3) has been extensively explored in kidney injury. The inhibition of EZH2 can alleviate AKI, tubulointerstitial fibrosis, and lupus nephritis, but potentiate podocyte injury in animal models, suggesting that the functional role of EZH2 varies with renal cell type and disease model[29]. Similarly, METTL10 is a lysine trimethyltransferase, encoded by gene *METTL10*, which has been reportedly identified as one of eGFR-associated genes and CKD risk genes[15-16]. Although emerging evidence have indicated the significance of lysine methylation on regulating renal function, limited studies have elucidated METTL10 in the regulation of renal function.

In this study, we first unveiled the downregulation of METTL10 in glomerular tissues of patients with with focal segmental glomerulosclerosis (FSGS) and in mice with Adriamycin (ADR)-induced nephropathy. Overexpression of METTL10 had a protective effect on injured podocytes by alleviateing dedifferention in vitro. Interestingly, recent studies indicate that many methyltransferases have multiple targets and plays unexpectedly pivotal roles in celular processes and diseases[30]. For instance, SETD2 methylates histone H3 as well as a growing list of non-histone proteins, including alpha-tubulin[31],and signal transducer and activator of transcription 1 (STAT1)[32]. *SETD2*is commonly mutated in renal cell carcinoma(RCC). Wang, TC et al. discovered that SETD2 is a key regulator of epithelial-to-mesenchymal transition (EMT) using different kidney epithelial cell lines[33]. Furthermore, Robert et al. explored SETD2-dependent changes in lysine methylation of proteins in proximal renal tubule cells, observing decreased lysine methylation of the translation elongation factor (eEF1A1) and loss of *METTL10*gene expression in SETD2-mutated kidney tumors[30].

eEF1A is an evolutionarily conserved nonhistone protein and extensively lysine-methylated proteins in eukaryotes, modulating mRNA translation. METTL10 mediates trimethylation of human eEF1A1 at lysine 318[13]. Recent studies have suggested that eEF1A methylation plays roles in aging biology via regulation of protein synthesis[14-34]. Although eEF1A methylation functions in the kidney remains unknown, increasing evidence suggestes that METTL proteins are more closely association with renal cancer risk than other cancers, indicating

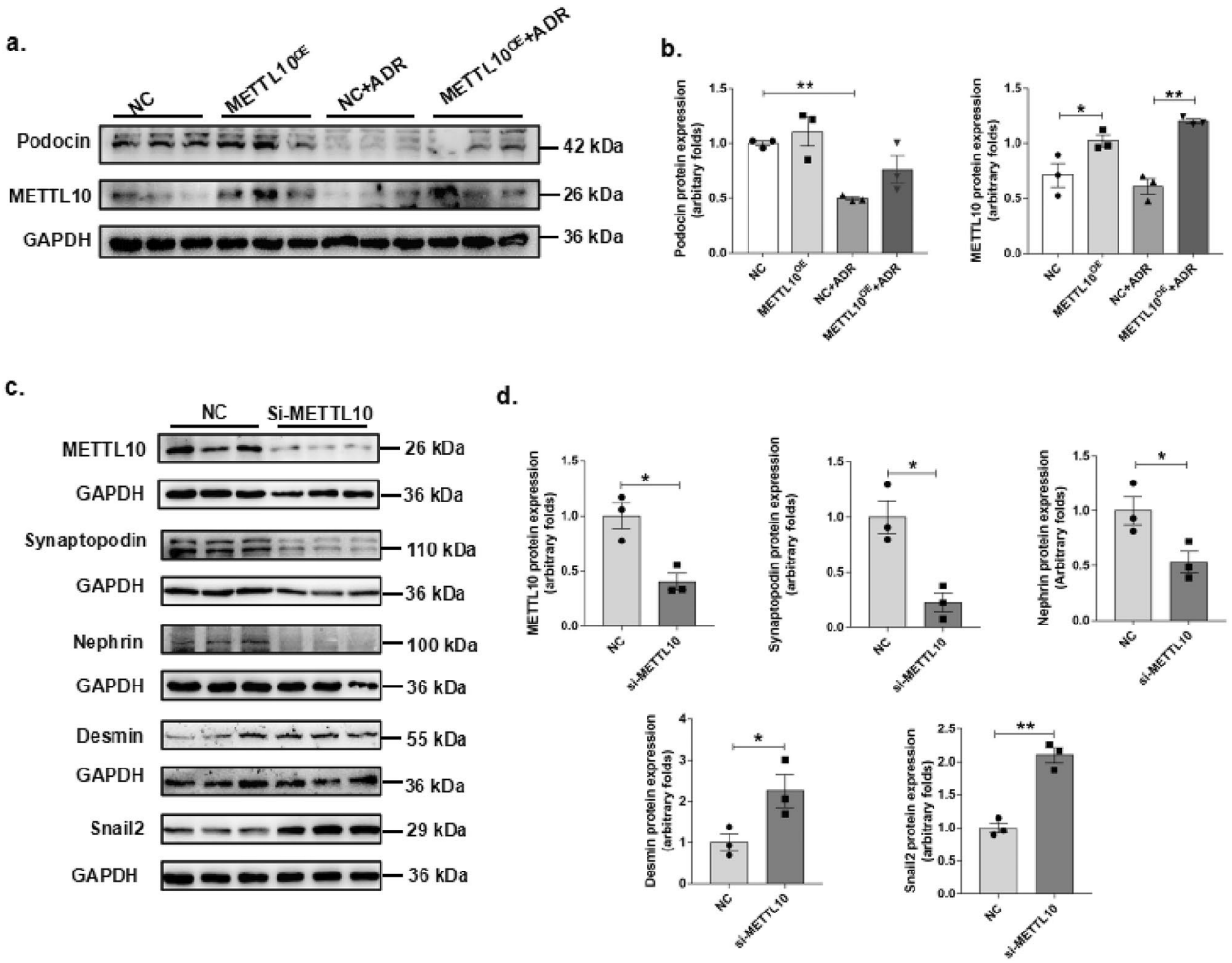

Fig. 4. Real-time PCR detection of related markers. mRNA expression of METTL10, podocyte markers and dedifferentiation-related genes examined by real-time PCR after ADR treatment for the indicated time periods. $n = 3$ per group. CON control, ADR adriamycin.b. Real-time PCR detection of the effect of METTL10 knockdown on podocyte markers and dedifferentiation-related genes. $n = 3$ per group. $^{*}P < 0.05$, NC negative control, si-METTL10 knockdown of METTL10.

a unique role of the METTL family in renal carcinoma[35]. Among these proteins, decreased expression of METTL10 is linked to decreased survival in patients with renal cancer[30]. METTL14 is reportedly downregulated in RCC and attenuates metastasis and EMT of RCC cells[36]. Notably, METTL14 has also been examined in proteinuric kidney diseases, including FSGS and DN[12-37]displaying a significantly protective effect on podocytes via activation of autophagy and inhibition of apoptosis and inflammation through posttranscriptional regulation of Sirt1 mRNA in vivo and in vitro[12]. However, few studies have explored whether METTL10 plays a similar role in FSGS and other glomerular diseases.

In the present study, we found that *METTL10* was one of the significantly downregulated differentially expressed genes (DEGs) in LMB2 (an immunotoxin)-induced podocyte injury (an experimental model of FSGS) in the GEO database. Similar to LMB2, ADR-induced nephropathy in mice is another common model to mimic human FSGS. We examined METTL10 expression in podocyte injury both in vivo and in vitro. Podocytes in glomeruli from human FSGS exhibited diminished METTL10 levels. Analogous to human disease, we observed that METTL10 levels in ADR-treated mice were reduced and negatively correlated with proteinuria. Similar to METTL14, we confirmed the downregulation of METTL10 in FSGS. Subsequently, we focused on the potential regulatory role of METTL10 in podocyte injury.

Podocyte dedifferentiation is considered an adaptive phenotypic change in podocytes after damage, similar to EMT in tubular cells injury, including loss of their molecular signatures (such as synaptopodin, nephrin, podocin, and WT-1) and acquisition of new mesenchymal markers[38-39]. This process induces loss of molecular signatures such as synaptopodin, nephrin, podocin, and WT-1, and acquisition of new mesenchymal markers, leading to podocyte damage, podocyte loss, and ultimately proteinuric glomerular diseases, including FSGS[40]. Recent investigations have uncovered that several lysine methyltransferases, such as EZH2, can alleviate podocyte dedifferentiation via trimethylation at histone H3 lysine 27 (H3K27), repressing the activation of Notch pathways

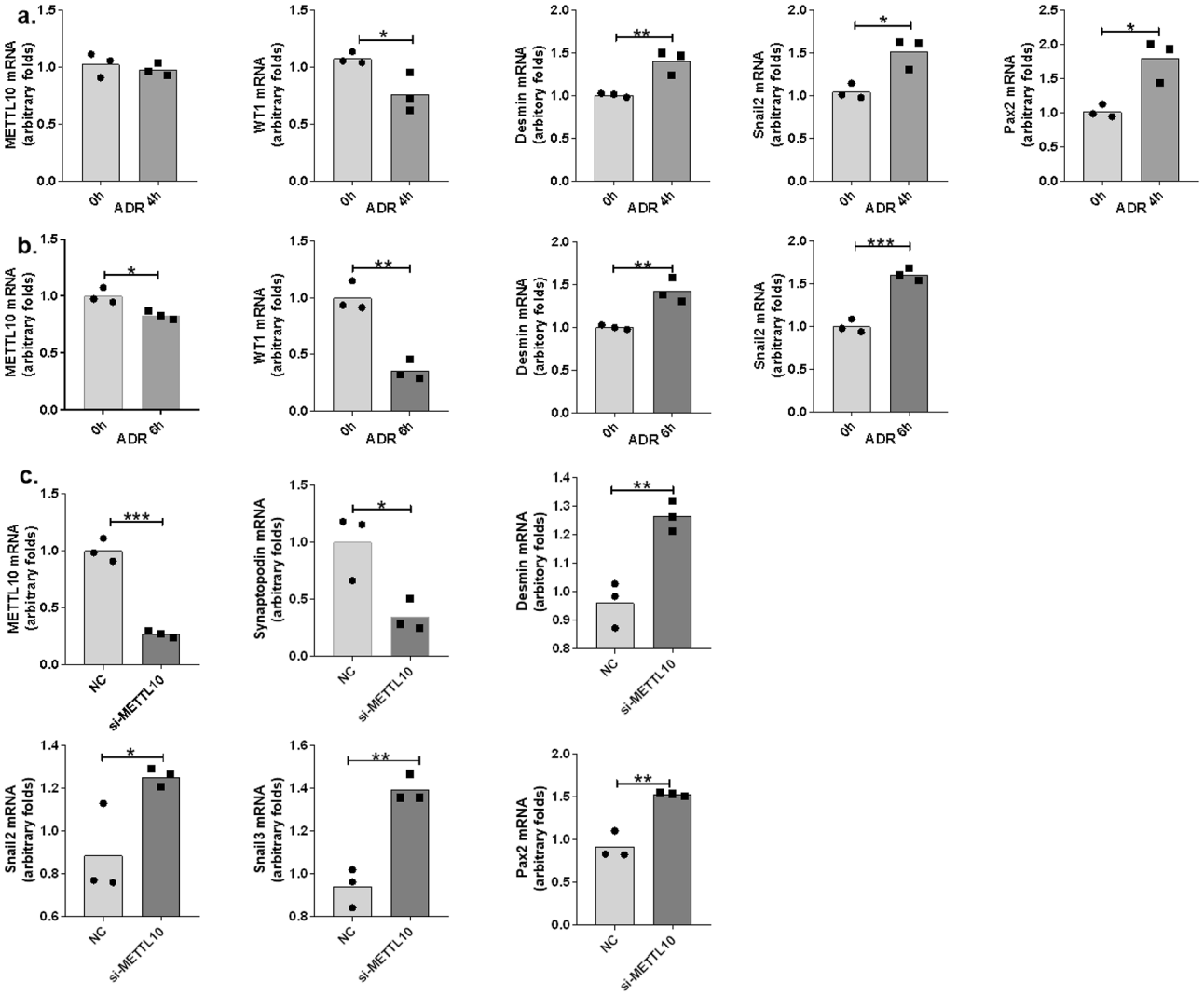

Fig. 5. METTL10 attenuated ADR-induced podocyte injury. (a) Podocytes were infected with lentivirus-METTL10-overexpression plasmids or negative control lentivirus, and the expression of METTL10 protein and podocin, a podocyte marker, was detected by western blotting. (b) Quantification of (a). $n = 3$ per group c-e. Knockdown of METTL10 promoted dedifferentiation of podocytes. (c) Immunoblotting assay of podocyte marker proteins and dedifferentiation-related proteins after transfection of METTL10-si RNA (small inference RNA). (d) Quantification of (c). $^{*}P < 0.05$, $^{**}P < 0.01$, $^{***}P < 0.001$. NC negative control, METTL10OE overexpression of METTL10, si-METTL10 knockdown of METTL10.

or the WT-1/ β-catenin pathway, thereby improving the outcomes of glomerular disease including FSGS and DN[41-42]. Therefore, we focused on the potential role of METTL10 in podocyte dedifferentiation under harmful conditions in vitro. METTL10 levels were reduced in cultured podocytes after ADR treatment, concomitant with podocyte dedifferentiation, manifested by decreased podocyte-specific markers such as podocin and WT-1 but increased expression of mesenchymal markers such as pax2, snail and desmin. Furthermore, the decrease in podocin stimulated by ADR was slightly reversed in METTL10-overexpressing podocytes. Additionally, METTL10 knockdown podocytes displayed enhanced expression of snail and desmin at the mRNA and protein levels. Since podocyte METTL10 downregulation was confirmed in podocyte injury and overexpression of METTL10 mitigated loss of podocin, we drew a tentative conclusion that METTL10 protects podocyte function partly by inhibiting dedifferentiation. Various pathways are involved in podocyte mesenchymal transition, including the cAMP-PKA pathway[40-43]. Therefore, we will further determine whether METTL10 modulates these dedifferentiation-related pathways.

However, there are several limitations in our present study. As far as we know, there are reportedly full supplies of commercial detecting kits for various histone lysine methylation. However, due to the lack of specific merchandise for detecting of lysine methylation levels of EEF1A1, it is challenging to examine the exact lysine methylatation on the eEF1A1 lysine 318, which could provide us with a more detailed mechanism for the role of METTL10 in pdocoyte injury. Recent advanced methodologies, such as chromatin immunoprecipitation, high-throughput DNA sequencing and RNA sequencing, could greatly help further identify the role of METTL10

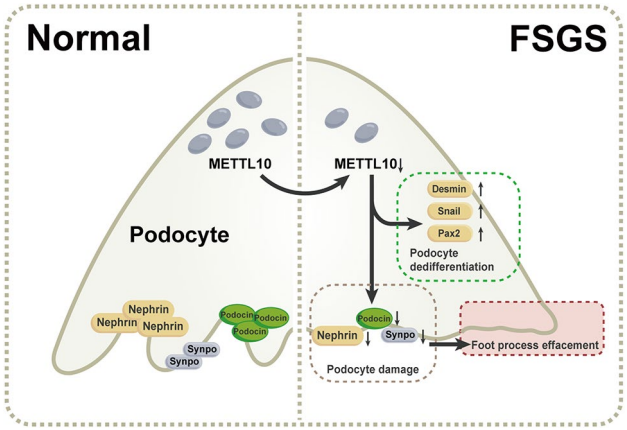

Fig. 6. Diagrammatic.

Reagents	Name of kit	Corporation	City	Country	Cat #
Adriamycin	Adriamycin	Sigma-Aldrich	St Louis	USA	D5220
Recombinant murine IFN-γ	Recombinant murine IFN-γ	PeproTech	Rocky Hill	USA	AF-315-05
Iron(III) oxide	Iron(III) oxide	Sangon Biotech	Shanghai	China	A502229-0250
Collagenase A	Collagenase A	Roche	Mannheim	Germany	10,103,578,001
Deoxyribonuclease I	Deoxyribonuclease I	ThermoFisher Scientific	Waltham	USA	18,047,019

Table 2. Reagents and category numbers.

as an EEF1A1 lysine trimethyltransferase for epigenetic modulation in podocyte injury. Second, in the present study, we explored the function of METTL10 in FSGS, considering that FSGS is a typical example of podocyte injury. However, METTL10 could play a vital role in different types of podocytopathies, not merely in FSGS. In the next step, we will extend the research to other podocytopathies, such as DN, and MN.

Collectively, these data suggest that METLL10, as a non-histone lysine trimethyltransferase, regulates podocyte dedifferentiation under harmful stimuli and partially protect podocytes from dedifferentiation. However, the exact mechanism by which METTL10-mediated eEF1A1 methylation play a role in podocyte dedifferentiation needs further study.

Materials and methods

Microarray data processing and differentially expressed gene identification. GSE108629, a microarray expression profile dataset related to a podocyte injury model, was downloaded from the GEO database (https://www.ncbi.nlm.nih.gov/gds/?).The dataset contained 8 samples: 4 normal specimens and 4 podocyte-injury samples induced by LMB2, a human (h)CD25-directed immunotoxin. The authentic array data were transformed into expression measures. Background correlation and data normalization were performed using principal component analysis (PCA) and boxplots. The limma package and affy package were used to identify differentially expressed genes (DEGs) between control samples and podocyte injury samples. Subsequently, the log2-fold change (log2 FC) was determined. Only those genes with $|\log FC| \geq 2$ and adjusted P value < 0.05 were regarded as DEGs.

Reagents

Adriamycin was purchased from Sigma Chemical (St Louis, MO, Cat#D5220). Recombinant murine IFN-γ was purchased from PeproTech (Rocky Hill, NJ, USA, Cat#AF-315-05). The iron oxide was purchased from Sangon Biotech(Shanghai, China, Cat#A502229-0250). Collagenase A was purchased from Roche (Mannheim, Germany, Cat#10103578001). Deoxyribonuclease I were from ThermoFisher Scientific ((Waltham, MA, USA, Cat#18047019). See more details in Table 2.

Human renal samples

Samples of renal biopsies were obtained from the Department of Nephrology, Renji Hospital, School of Medicine, Shanghai Jiaotong University. Stored former kidney biopsy samples were searched cautiously from January 2019 to January 2020. The inclusion criteria of FSGS were as follows. (1) 24-h urinary protein was > 3.5 g/24 h. (2) The histopathological lesion was focal segmental glomerulosclerosis (FSGS). The eGFR was > 90 mL·(min·1.73 m2) −1. The control samples were obtained from the healthy kidney poles of individuals who underwent tumor nephrectomies without a history of diabetes or chronic kidney diseases. Patient clinical data (sex, age, disease history and physical examination) and laboratory data (serum creatinine, BUN, eGFR levels and 24-h urinary protein) were collected. The investigation was conducted according to the principles of the Declaration of

Helsinki and was approved by the Research Ethics Committee of Renji Hospital (IRB approval number 2017-084). Informed consent was obtained from all participants.

Immunofluorescence staining

Paraffin-embedded, 4-μm thick sections were fixed in 4% paraformaldehyde for 15 min. After blocking, the paraffin-embedded sections were incubated with primary antibodies and then with a fluorescein Cy3-FITC-labeled secondary antibody (1:100; Servicebio Wuhan, China; Cat# SA00009-2). Fluorescence images were recorded using fluorescence microscopy (Zeiss, Axio Vert A1). The following primary antibodies were used: anti-METTL10 (1:100; Biorbyt, Cambridge, Britain; Cat#orb1880812) and anti-podocalyxin (1:1500; Proteintech, Wuhan, China; Cat#18150-1-AP). Podocytes were seeded onto a clean glass coverslip, fixed with 4% paraformaldehyde, and then penetrated with 0.2% Triton X-100. The slide was incubated with anti-METTL10 antibody (1:100; Biorbyt, Cambridge, Britain; Cat#orb1880812).

Animal experiments

All animal procedures performed were approved by the Animal Care Committee at Renji Hospital, School of Medicine, Shanghai Jiao Tong University and complied with the ethical regulations of the Animal Protocol Committee of Shanghai Jiao Tong University. This study was carried out in compliance with the ARRIVE guidelines. Male BALB/C mice (Shanghai Slac Laboratory Animal, China) aged 6–8 weeks were divided into a control group and an ADR-model group. ADR nephropathy was induced by a single intravenous injection of ADR at 10 mg/kg body weight[44]. On Days 0 and 14, urine was collected for 24 h using a metabolic cage ($n=5$ per group). On Day 15, mice were sacrificed under pentobarbital sodium anesthesia. Kidneys were removed for analyses.

Electron microscopy

For transmission electron microscopy, the kidney tissues were dissected into 1–2 mm sections, immediately fixed in 2.5% PBS-buffered glutaraldehyde for 2 h, postfixed in 1% osmium tetroxide for 2 h, dehydrated in graded ethanol, and embedded in Epon 812. Ultrathin sections for ultrastructural examination were double-stained with uranyl acetate and lead citrate and examined via transmission electron microscopy (H-7650; Hitachi, Tokyo, Japan). Podocyte foot process effacement was analyzed.

Measurement of urine albumin/creatinine ratio

Urine albumin and creatinine concentrations were determined using an albumin assay kit and a creatinine assay kit (Jiancheng, Nanjing, China). For the quantification of urine albumin and creatinine, the absorbance was determined at 628 nm and 546 nm, respectively, using a microplate reader.

Isolation of Glomeruli

Mouse glomeruli were isolated as described[45].Briefly, mice were perfused with 40 ml HBSS containing 2.5 mg/ml iron oxide and 0.1% BSA through the heart. At the end of perfusion, kidneys were removed, minced into 1 mm^3 pieces, and digested in HBSS containing 1 mg/ml collagenase A and 100 U/ml deoxyribonuclease I at 37 °C for 30 min with gentle agitation. During the following procedure, kidney tissues were kept at 4 °C. The digested tissue was gently pressed through two 100 μm cell strainers and the cell strainers were washed with 10 ml of HBSS for twice. The cell suspension was then centrifuged at 200 g for 5 min. The supernatant was discarded and the cell pellet was resuspended in 2 ml of HBSS. Finally, glomeruli containing iron oxide were collected by a magnetic particle concentrator and washed for three to five times with HBSS. The purity of glomeruli was verified under microscopy.

Cell culture

Conditionally immortalized mouse podocytes were kindly provided by Dr Peter Mundel and were cultured as described previously[46]. The cell line has been used in our previous studies[47–50]. In brief, podocytes proliferate under growth permissive conditions at 33℃ in RPMI 1640 with 10% FBS, 10 U/ml mouse recombinant interferon-γ (IFN-γ), and 100 U/ml penicillin plus 0.1 mg/ml streptomycin. For differentiation, these cells were then maintained in nonpermissive conditions at 37 °C without IFN-γ for 10–14 days and were then treated with various reagents. The majority of the cells had an arborous shape and expressed synaptopodin. All experiments were replicated at least three times for the indicated conditions. Podocytes between passages 15 and 25 were used in the experiments.

Western blotting assay

Total protein was extracted from the mouse glomerula and a mouse podocyte cell line. For tissue lysis, the mouse glomerula isolated were diced into pieces with a scalpel and added to ice-cold RIPA buffer containing steel balls (RIPA Lysis Buffer SystemSanta Cruz Biotechnology, Cat# sc-24948). Subsequently, transfer the tissue preparation to automatic sample fast grinder (Shanghai Jingxin, China) on ice for 180 s and crudely clear the extracts by centrifugation at 12,000 g at 4℃ for 1 min. For cell lysis, the podocytes were washed by 1× ice-cold PBS. Either tissue or cell preparation was lysed in RIPA buffer, followed with a 30-minute incubation on ice. Finally the lysates were collected after centrifugation at 12,000 g for 15 min at 4℃. The protein concentration was determined using a bicinchoninic acid reagent (Thermo Scientific, Cat# A65453). Protein samples were resolved by SDS–PAGE and transferred to a nitrocellulose membrane. The antibodies used were anti-METTL10 (1:200, Thermo Scientific; Cat# PA5-69581), anti-podocin D(1:500, Proteintech; Cat# 20384-1-AP), anti-synaptopodin (1:500, Proteintech; Cat# CL488-21064), anti-WT1 (1:500, Proteintech; Cat# 12609-1-AP), anti-nephrin (1:200, Abcam; Cat# ab216692), anti-desmin (1:500, Proteintech; Cat# 16520-1-AP), anti-snail2 (1:500, Proteintech;

Item	Control group($n=4$)	FSGS group($n=6$)
Age/year	63.00 ± 15.02	31.17 ± 15.72
Gender/*n*		
Male	1	4
Female	3	2
Blood pressure/mmHg		
Systolic	133.5 ± 14.62	114.50 ± 12.68
Diastolic	81.00 ± 6.93	75.67 ± 9.61
Urine protein for 24 h/g	/	7.38 ± 2.56**
ALB/ ($g.L^{-1}$)	42.78 ± 7.15	26.06 ± 7.07**
sCr /($\mu mol \cdot L^{-1}$)	50.65 ± 4.01	71.57 ± 15.11
BUN/($mmol \cdot L^{-1}$)	5.05 ± 1.79	4.95 ± 2.22
eGFR/[$mL \cdot (min \cdot 1.73m^2)^{-1}$]	103 30 ± 11.00	113.20 ± 18.78

Table 3. Demographic and baseline characteristics of control group and FSGS group. Plus-minus values are mean ± SD; $^{**}P < 0.01$; eGFR, estimated glomerular filtration rate; BUN, blood urea nitrogen; sCr, serum creatine; ALB, Serum albumin.

Cat# 12129-1-AP), anti-tubulin (1:1000, Beyotime, Shanghai, China; Cat# AF2827) and anti-GAPDH (1:2000, Cell Signaling Technology; Cat# 2118).Immunoblot bands were visualized using a Tanon imaging system (Zhejiang, China). Target protein band densitometric quantification was performed using Image J software and normalized to loading controls and GAPDH levels .

Quantitative real-time PCR (qPCR)

Total RNA was extracted from cells by an EZ-press RNA Purification kit (EZBioscience, Beijing, China, Cat# B0004DP) according to the manufacturer's instructions. The concentration of extracted RNA was determined by calculating absorbance at wavelengths of 260 nm (A260) and 280 nm (A280) by NanoDrop2000 (Thermo Scientific, USA). cDNA was synthesized using the PrimeScript RT reagent Kit (TaKaRa Bio, Japan), and then, cDNA samples were denatured and amplified using a Light Cycler 480 real-time PCR system (Roche Applied Science, Mannheim, Germany). Each target gene was amplified by 40 cycles. All specimens were tested with three replicates and their melting curves were analyzed. All target genes mRNA expression was normalized to GAPDH by the 2 -ΔΔCt (Livak) method. Exactly, the relative expression was calculated via the following equation: $RQ = 2^{-(\Delta Ctq - \Delta Ctcb)}$,

where ΔCtq is the difference of the average Ct values between the target gene and GAPDH in the test Group, while ΔCtcb is the difference between the target gene and GAPDH in the control group. PCR primers were synthetized by Sangon Biotech (Shanghai, China), and the sequences are shown in Table 3.

LentiORF-METTL10 overexpression and RNA interference

The LentiORF-METTL10 clone was purchased from Zuorun Company (Shanghai, China), and stable METTL10 overexpression was achieved by infecting mouse podocytes using lentivirus produced from HEK 293T cells. Cells expressing GFP were selected with puromycin for 2 days before use in all studies. GFP expression and Western blotting were performed to confirm METTL10 overexpression in lentiORF-METTL10 compared with lentiORF-GFP mouse podocytes. METTL10 small interfering RNA (siRNA) (sense: 5'-GAGUAUGAACCGA CUAAUATT-3' and antisense: 5'-UAUUAGUCGGUUCAUACUCTT-3') and a negative control siRNA were purchased from Zuorun Company (Shanghai, China). siRNAs (50 nmol/L) were transiently transfected using Lipofectamine 3000 (Thermo Scientific, USA) according to the manufacturer's instructions. Approximately 24–48 h after siRNA infection, q-PCR and western blotting were used to evaluate the suppression of METTL10 expression in different cell groups.

Statistical analysis

Quantitative data are representative of at least three experiments. Statistical analyses were performed by GraphPad Prism 7 (GraphPad Software, Inc.). Experimental results with a normal distribution are depicted as the mean ± standard error of the mean (SEM); clinical data with a normal distribution are presented as the mean ± standard deviation (SD). An unpaired Student's t test was used to analyze the difference between two groups, and one-way analysis of variance with Tukey's test was used for multiple comparisons. Spearman correlation analysis was used to assess the coefficient (r) and P value between METTL10 expression and the urinary albumin/creatine ratio in all mice. Linear regression was performed to depict the linear relationship. Only P values < 0.05 were considered statistically significant.

Data availability

The datasets used and/or analyzed during the current study are available from the corresponding author on reasonable request. The datasets supporting the conclusions of this article are included within the article.

Received: 3 March 2024; Accepted: 19 November 2024

Published online: 07 January 2025

References

1. Ko, Y. A. et al. Genetic-variation-driven gene-expression changes highlight genes with important functions for kidney disease. *Am. J. Hum. Genet.* **100**, 940–953 (2017).
2. Ayodele, O. E. & Alebiosu, C. O. Burden of chronic kidney disease: an International Perspective. *Adv. Chronic Kidney Dis.* **17**, 215–224 (2010).
3. Zuo, Y. et al. Identification of Matrix Metalloproteinase-10 as a key mediator of Podocyte Injury and Proteinuria. *Kidney Int.* **100**, 837–849 (2021).
4. Jiang, H. et al. Understanding the Podocyte Immune responses in proteinuric kidney diseases: from pathogenesis to Therapy. *Front. Immunol.* **14**, 1335936 (2023).
5. Shankland, S. J., Jefferson, J. A. & Wessely, O. Repurposing Drugs for Diseases Associated with Podocyte Dysfunction. *Kidney Int.* **104**, 455–462 (2023).
6. Yamamoto-Nonaka, K. et al. Cathepsin D in Podocytes is important in the pathogenesis of Proteinuria and Ckd. *J. Am. Soc. Nephrol.* **27**, 2685–2700 (2016).
7. Yang, J. W. et al. Recent advances of animal model of focal segmental glomerulosclerosis. *Clin. Exp. Nephrol.* **22**, 752–763 (2018).
8. Lee, V. W. & Harris, D. C. Adriamycin nephropathy: a model of focal segmental glomerulosclerosis. *Nephrology* **16**, 30–38 (2011).
9. Bhat, K. P., Umit, K. H., Jin, J. & Gozani, O. Epigenetics and Beyond: Targeting writers of protein lysine methylation to treat Disease. *Nat. Rev. Drug Discov.* **20**, 265–286 (2021).
10. Yin, J., Qi, T. F., Li, L. & Wang, Y. Targeted profiling of Epitranscriptomic Reader, Writer, and Eraser proteins regulated by H3K36Me3. *Anal. Chem.* **95**, 9672–9679 (2023).
11. Liu, Z., Chen, Y. & Shen, T. Evidence based on an Integrative Analysis of Multi-omics Data on Mettl7a as a molecular marker in Pan-cancer. *Biomolecules.* **13(2),** 195 (2023).
12. Lu, Z. et al. Mettl14 aggravates Podocyte Injury and Glomerulopathy Progression through N(6)-Methyladenosine-dependent downregulating of Sirt1. *Cell. Death Dis.* **12**, 881 (2021).
13. Jakobsson, M. E., Małecki, J. & Falnes, P. Ø. Regulation of eukaryotic elongation factor 1 alpha (Eef1a) by dynamic lysine methylation. *Rna Biol.* **15**, 314–319 (2018).
14. Abbas, W., Kumar, A. & Herbein, G. The Eef1a proteins: at the crossroads of Oncogenesis, apoptosis, and viral infections. *Front. Oncol.* **5**, 75 (2015).
15. Hellwege, J. N. et al. Mapping Egfr loci to the renal transcriptome and phenome in the va million veteran program. *Nat. Commun.* **10**, 3842 (2019).
16. Sheng, X. et al. Systematic Integrated Analysis of Genetic and Epigenetic Variation in Diabetic kidney disease. *Proc. Natl. Acad. Sci. U S A.* **117**, 29013–29024 (2020).
17. Rane, M. J., Zhao, Y. & Cai, L. Krüppel-Like factors (Klfs) in renal physiology and disease. *Ebiomedicine* **40**, 743–750 (2019).
18. Campeanu, I. J. et al. Multi-omics Integration of Methyltransferase-Like Protein Family reveals clinical outcomes and functional signatures in Human Cancer. *Sci. Rep.* **11**, 14784 (2021).
19. Herman-Edelstein, M., Weinstein, T. & Gafter, U. Tgfβ1-Dependent podocyte dysfunction. *Curr. Opin. Nephrol. Hypertens.* **22**, 93–99 (2013).
20. Jiang, L. et al. Calmodulin-dependent protein kinase II/Camp Response element-binding Protein/Wnt/B-Catenin Signaling Cascade regulates angiotensin II-Induced Podocyte Injury and Albuminuria. *J. Biol. Chem.* **288**, 23368–23379 (2013).
21. Ma, T. et al. High glucose induces Autophagy in Podocytes. *Exp. Cell. Res.* **319**, 779–789 (2013).
22. Hartleben, B. et al. Autophagy influences glomerular Disease susceptibility and maintains Podocyte Homeostasis in Aging mice. *J. Clin. Invest.* **120**, 1084–1096 (2010).
23. Liu, Y. New insights into epithelial-mesenchymal transition in kidney fibrosis. *J. Am. Soc. Nephrol.* **21**, 212–222 (2010).
24. Zeng, C. et al. Podocyte Autophagic Activity plays a protective role in Renal Injury and Delays the Progression of Podocytopathies. *J. Pathol.* **234**, 203–213 (2014).
25. Relle, M. et al. New perspectives on the renal slit diaphragm protein podocin. *Mod. Pathol.* **24**, 1101–1110 (2011).
26. Meliambro, K., He, J. C. & Campbell, K. N. Podocyte-targeted therapies - progress and future directions. *Nat. Rev. Nephrol.* **20**(10), 643–658 (2024).
27. Bhat, K. P., Ümit, K. H., Jin, J. & Gozani, O. Epigenetics and Beyond: Targeting writers of protein lysine methylation to treat Disease. *Nat. Rev. Drug Discov.* **20**, 265–286 (2021).
28. Jin, J., Liu, X. M., Shao, W. & Meng, X. M. Nucleic acid and protein methylation modification in Renal diseases. *Acta Pharmacol. Sin.* **45**, 661–673 (2024).
29. Li, T., Yu, C. & Zhuang, S. Histone methyltransferase Ezh2: a potential therapeutic target for kidney diseases. *Front. Physiol.* **12**, 640700 (2021).
30. Hapke, R. et al. Setd2 regulates the methylation of translation elongation factor Eef1a1 in Clear Cell Renal Cell Carcinoma. *Kidney Cancer J.* **6**, 179–193 (2022).
31. Walker, C. & Burggren, W. Remodeling the Epigenome and (Epi)Cytoskeleton: a New Paradigm for Co-regulation by methylation. *J. Exp. Biol.* **223**(Pt 13), jeb220632 (2020).
32. Chen, K. et al. Methyltransferase Setd2-Mediated methylation of Stat1 is critical for Interferon Antiviral Activity. *Cell* **170**, 492–506 (2017).
33. Wang, T. et al. Setd2 loss in renal epithelial cells drives epithelial-to-mesenchymal transition in a Tgf-B-Independent manner. *Mol. Oncol.* **18**, 44–61 (2024).
34. Mealey-Farr, R. et al. Antibody Toolkit to investigate Eef1a methylation Dynamics in Mrna Translation Elongation. *J. Biol. Chem.* **299**, 104747 (2023).
35. Yang, Z. et al. The Novel putative methyltransferase Mettl7a as one Prognostic Biomarker potentially Associated with Immune Infiltration in Human Renal Cancer. *Heliyon* **9**, e15371 (2023).
36. Liu, Z., Sun, T., Piao, C., Zhang, Z. & Kong, C. Mettl14-Mediated N(6)-Methyladenosine modification of Itgb4 Mrna inhibits metastasis of Clear Cell Renal Cell Carcinoma. *Cell. Commun. Signal.* **20**, 36 (2022).
37. Li, M., Deng, L. & Xu, G. Mettl14 promotes glomerular endothelial cell Injury and Diabetic Nephropathy Via M6a modification of A-Klotho. *Mol. Med.* **27**, 106 (2021).
38. Benedetti, V. et al. Alteration of thyroid hormone signaling triggers the Diabetes-Induced pathological growth, remodeling, and dedifferentiation of Podocytes. *Jci Insight,* **4**(18), e130249 (2019).
39. Kumar, V. et al. Disrupted apolipoprotein L1-Mir193a Axis dedifferentiates podocytes through Autophagy Blockade in an Apol1 risk milieu. *Am. J. Physiol. Cell. Physiol.* **317**, C209–C225 (2019).
40. Chang, K. et al. Ep300/Cbp is crucial for Camp-Pka Pathway to Alleviate Podocyte Dedifferentiation Via Targeting Notch3 Signaling. *Exp. Cell. Res.* **407**, 112825 (2021).
41. Majumder, S. et al. Shifts in podocyte histone H3K27Me3 regulate mouse and human glomerular disease. *J. Clin. Invest.* **128**, 483–499 (2018).
42. Wan, J. et al. Wt1 ameliorates Podocyte Injury Via repression of Ezh2/Beta-Catenin pathway in Diabetic Nephropathy. *Free Radic Biol. Med.* **108**, 280–299 (2017).

43. Zhu, X., Zhang, C., Liu, L., Xu, L. & Yao, L. Senolytic Combination of Dasatinib and Quercetin protects against Diabetic kidney disease by activating autophagy to Alleviate Podocyte Dedifferentiation Via the Notch Pathway. *Int. J. Mol. Med.* **53**(3), 26 (2024).
44. Awad, A. S. et al. Activation of Adenosine 2a receptors preserves structure and function of Podocytes. *J. Am. Soc. Nephrol.* **19**, 59–68 (2008).
45. Takemoto, M. et al. A New Method for large scale isolation of kidney glomeruli from mice. *Am. J. Pathol.* **161**, 799–805 (2002).
46. Mundel, P., Reiser, J. & Kriz, W. Induction of differentiation in cultured rat and human podocytes. *J. Am. Soc. Nephrol.* **8**, 697–705 (1997).
47. Xie, K. et al. Yes-Associated protein regulates Podocyte Cell Cycle Re-entry and Dedifferentiation in Adriamycin-Induced Nephropathy. *Cell. Death Dis.* **10**, 915 (2019).
48. Xie, K. et al. Protein kinase a/Creb Signaling prevents Adriamycin-Induced Podocyte apoptosis Via Upregulation of mitochondrial respiratory chain complexes. *Mol. Cell. Biol.* **38**(1), e00181–17 (2018).
49. Tao, H. et al. Cyclic amp prevents decrease of Phosphorylated Ezrin/Radixin/Moesin and Chloride Intracellular Channel 5 expressions in injured podocytes. *Clin. Exp. Nephrol.* **19**, 1000–1006 (2015).
50. Li, X. et al. Camp Signaling prevents Podocyte apoptosis Via activation of protein kinase a and mitochondrial Fusion. *Plos One*. **9**, e92003 (2014).

Author contributions

J.B. and L.W. conceived and designed the research; J.B., Z.L., H.Y., and B.W. performed the experiments; J.B. analyzed the data; J.B., L.G. and L.W. interpreted the results of the experiments; J.B. drafted the manuscript; L.W. and Y.P. edited and revised the manuscript; L.W. approved the final version of the manuscript.

Funding

This study was supported by the Shanghai Municipal Science and Technology Commission (No. 19ZR1430800), the Science and Technology Development Fund of Shanghai Pudong New Area (Grant No. PKJ2021-Y37), the Natural Science Foundation of China (Project no. 82170715) and the Talents Training Program of Pudong Hospital affiliated with Fudan University (Project no. LJ202201).

Declarations

Conflict of interest

The authors have no conflicts of interest to declare.

Additional information

Supplementary Information The online version contains supplementary material available at https://doi.org/10.1038/s41598-024-80526-8.

Correspondence and requests for materials should be addressed to L.W.

Reprints and permissions information is available at www.nature.com/reprints.

Publisher's note Springer Nature remains neutral with regard to jurisdictional claims in published maps and institutional affiliations.

Open Access This article is licensed under a Creative Commons Attribution-NonCommercial-NoDerivatives 4.0 International License, which permits any non-commercial use, sharing, distribution and reproduction in any medium or format, as long as you give appropriate credit to the original author(s) and the source, provide a link to the Creative Commons licence, and indicate if you modified the licensed material. You do not have permission under this licence to share adapted material derived from this article or parts of it. The images or other third party material in this article are included in the article's Creative Commons licence, unless indicated otherwise in a credit line to the material. If material is not included in the article's Creative Commons licence and your intended use is not permitted by statutory regulation or exceeds the permitted use, you will need to obtain permission directly from the copyright holder. To view a copy of this licence, visit http://creativecommons.org/licenses/by-nc-nd/4.0/.

© The Author(s) 2024